www.czasopisma.pan.pl PAN POLSKA AKADEMIA NAUK www.journals.pan.pl

Arch. Metall. Mater. **63** (2018), 4, 1715-1723

DOI: 10.24425/amm.2018.125097

SHIH-HSIEN CHANG*#, CHIEN-LUN LI*, KUO-TSUNG HUANG**, TZU-HSIEN YANG*#

EFFECT OF VACUUM HOT-PRESS PROCESS ON THE SINTERED CHARACTERISTICS AND MECHANICAL PROPERTIES OF A HIGH-DENSITY Cr-31.2 MASS% Ti ALLOY

In this study, two different compositions of submicron-structured titanium (760 nm) and micron-structured chromium (4.66 μm) powders were mixed to fabricate Cr-31.2 mass% Ti alloys by vacuum hot-press sintering. The research imposed various hot-press sintering pressures (20, 35 and 50 MPa), while the sintering temperature maintained at 1250°C for 1 h. The experimental results showed that the optimum parameters of the hot-press sintered Cr-31.2 mass% Ti alloys were 1250°C at 50 MPa for 1 h. Also, the relative density reached 99.94%, the closed porosity decreased to 0.04% and the hardness and transverse rupture strength (TRS) values increased to 81.90 HRA and 448.53 MPa, respectively. Moreover, the electrical conductivity is enhanced to $1.58 \times 10^4\ S \cdot cm^{-1}$. However, the grain growth generated during the high-temperature and high-pressure of the hot-press sintering process resulted in the grain coarsening phenomenon of the Cr-31.2 mass% Ti alloys after 1250°C hot-press sintering at 50 MPa for 1 h. In addition, the Cr-31.2 mass% Ti alloys were fabricated with the submicron-structured titanium (760 nm) and chromium (588 nm) powders showed more effective compaction than the micron-structured titanium (760 nm) and chromium (4.66 μm) powders did. The closed porosity decreases to 0.02% and the hardness values increase to 83.23 HRA. However, the agglomeration phenomenon of the Cr phase and brittleness of the $TiCr_2$ Laves phases easily led to a slight decrease in TRS (400.54 MPa).

Keywords: Cr-31.2 mass% Ti alloy, vacuum hot-press sintering, relative density, TRS and electrical conductivity

1. Introduction

Titanium (Ti) alloys are one of the most important engineering materials that are well known for their excellent specific strength and corrosion resistance. These are extensively used in a wide variety of applications including aerospace components, sporting goods and medical devices [1]. Chromium (Cr) element is suitable for alloying with titanium according to the following reasons. For example, Cr element can balance the anodic activity of the alloy and increases the passivation tendency of Ti alloys. The additional Ti element to Cr alloy takes advantage of reducing the liquidus temperature gradually from the high melting point of pure Ti (1670°C) to minimum temperature (1410°C) with Cr element adding and approaching the content of 46% [2]. Hence, Cr element is optimal element as an additional element for developing Cr-Ti alloy based biomaterials.

Cr-Ti alloys have been the object of great research interest due to their promising high temperature strength, excellent wear resistance, good oxidation resistance, as well as electrical properties and hydrogen solubility [3,4]. For a Cr-Ti binary alloy system, the BCC crystal structure is a metastable phase at room temperature. The stable phases in $TiCr_2$ alloy at room temperature are the mixture Lave phase of C14 and C15 structures [5]. Recently, Cr-based Laves phases have also been investigated for high temperature structural applications due to their high melting point, high strength and reasonably good oxidation resistance at elevated temperatures [6].

The chromium-titanium alloys formed Laves phase $TiCr_2$ intermetallic compounds. Cr and refractory metals were used to form XCr_2 (X is Ti, Nb, Ta, Zr and Hf, etc.) which preforms the material characteristic with a high melting point and the appropriate density. When Cr-Ti alloys have an amount of Cr led to stay at stable state of the intermetallic phase, these alloy compounds have advantage of good high-temperature oxidation resistance, high temperature stress strength, anti-creep deformation capability and excellent against thermal corrosion. These compound materials were used to apply for the field of aerospace parts due to their high structural strength aiming to endure and exceed a high temperature environment of 1200°C.

In addition, when the chromium-titanium alloy applied to a sputtering target material, the Cr-Ti thin film deposited by sputtering had high hardness, good oxidation resistance and high wear resistance, and can be applied to a protective layer on the surface of a tool or mould to extend its life [7,8]. Laves phase $TiCr_2$ also has the potential to perform in hydrogen storage battery and be worth to notice [9].

Generally speaking, titanium and its alloys can be produced by conventional processes, like casting, and by powder metal-

* NATIONAL TAIPEI UNIVERSITY OF TECHNOLOGY, DEPARTMENT OF MATERIALS AND MINERAL RESOURCES ENGINEERING, TAIPEI 10608, TAIWAN, ROC
** NATIONAL KANGSHAN AGRICULTURAL INDUSTRIAL SENIOR HIGH SCHOOL, DEPARTMENT OF AUTO-MECHANICS, KAOHSIUNG 82049, TAIWAN, ROC
# Corresponding authors: changsh@ntut.edu.tw, yangdavid180@gmail.com

lurgy (P/M) where powders are consolidated and sintered to produce near-net-shape products. However, the parts usually suffer from residual porosity. In order to improve this disadvantage, alternative processes, where the sintering step is carried out simultaneously with the application of high temperature and pressure, were developed [10]. The hot-press sintering is an effective way to fabricate materials with relatively high density. It is usually used to improve the sintering quality [11]. This technique provides an additional axial pressure that aids in decreasing the sintering temperature and promoting the densification of materials. In recent years, hot-press sintering technique is the most commonly used methods for preparing ceramics and alloys [12-14].

Conventional P/M involves mixing the metal powders, compacting of the mixed powders into molds and then sintering of the compact powders under the different atmospheres [15,16]. As mentioned previously, P/M is a good method for fabrication of high melting material (ex Cr and Ti) with excellent mechanical properties. It offers two different types of materials with the objective of achieving higher strength, hardness and wear resistance [16-18]. Among them, the hot-press sintering is another special P/M technology, it can obtain the dense material at a relatively lower sintering temperature [15-19]. In the present research, a Cr-Ti alloy was fabricated by means of the vacuum hot-press sintering process of P/M technology. Recently, the research also focused on the examination of the sintering behavior in the field of the Cr alloys and its phase equilibrium diagram [20-22].

The motivation of this study was for increasing the relative density of Cr-31.2 mass% Ti alloys although a great deal of effort has been made so far. However, what seems to be lacking was improving the mechanical characterization in progress. So, the aim of this study was to investigate the optimal parameters of micron-(Cr) and submicron-(Ti) Cr-31.2 mass% Ti alloys by using hot-press sintering technology. Besides, in order to evaluate the effect of the particle size of the Cr powders, the submicron-structured titanium (760 nm) and chromium (588 nm) powders were mixed, and Cr-31.2 mass% Ti alloys were produced via an optimal hot-press sintering procedure. A series of experiments on the specimens of hot-press sintering at different pressures were simultaneously carried out to explore the sintering characteristics of the Cr-31.2 mass% Ti alloys. The influence of the microstructural features on the mechanical and electrical conductivity properties was also investigated.

2. Experimental procedure

In this work, 99.95% submicron-structured titanium (760 nm) and micron-structured chromium (4.66 μm) powders were mixed and Cr-31.2 mass% Ti alloys fabricated via the powder metallurgy (P/M) technique. The powders were mixed by the planetary ball mill (ITOH Co., LP-1). The number of revolutions was 300 rpm for 1 h, and the medium adopted tungsten carbide ball. The research imposed various hot-pressing pressures 20, 35 and 50 MPa, respectively, while the temperature was maintained at 1250°C for 1 h. Meanwhile, the value of the pump vacuumed at 1.33×10^{-1} Pa. And, the size of vacuum hot-presses sintering compact was $40 \times 40 \times 5$ mm^3. Microtrac X 100 laser instrument was used to analyze the particle size of the micron and submicron-size powders. The mean particle sizes of the reduced micron and submicron-structured chromium powders were 4.66±0.32 μm and 588±21 nm, respectively, and the mean particle size of the reduced submicron-structured titanium powder was 760±41 nm.

In the experimental procedure, the experiments performed to evaluate the sintered characteristics of the Cr-31.2 mass% Ti alloys through various pressures of hot-press sintering (Yu Tai Vacuum Co., Ltd. HPS-1053) pressures, the porosity, relative density, hardness, transverse rupture strength (TRS), and electrical tests. Microstructural features and morphology of the specimens were examined by X-ray diffraction (XRD, Rigaku D/Max-2200) and observed by the scanning electron microscopy (SEM, Hitachi-S4700). Porosity tests followed the ASTM B311-08 and C830 standards, and the closed porosity measurements were carried out through the analysis software of Image Pro. Besides, the sintered density was calculated by the Archimedes Method, and followed the ASTM B311-13 standard. Meanwhile, the relative density (R.D.) was calculated by the equation: closed porosity + open porosity + relative density = 100%.

The hardness of the specimens was measured by Rockwell indenter (HRA, Indentec 8150LK) with loading of 588.4 N, which complied with the CNS 2114 Z8003 standard methods. And, R_{bm} was the transverse rupture strength (TRS), which determined as the fracture stress in the surface zone. F was maximum fracture load, L was 30 mm, k was a chamfer correction factor (normally 1.00-1.02), b and h were 5 mm in the equation $R_{bm} = 3FLk/2bh^2$, respectively. The specimen dimensions of the TRS test were $5 \times 5 \times 40$ mm^3. A four-point probe (LRS4-TG2) was used to measure sheet resistance. In addition, electrical conductivity (σ) was calculated according to the following formula [15]:

$$\rho = R/t = 1/\sigma$$

Where the ρ is electrical resistivity, R is the resistance, t is the thickness of the test sheet, and σ is the electrical conductivity ($S \cdot cm^{-1}$), respectively.

3. Results and discussion

Figure 1 shows the XRD patterns of the Cr-31.2 mass% Ti alloys after the hot-press sintering process at various pressures. According to our previous studies [15,16], the Cr (110) intensity of the Cr-based alloys was obviously enhanced as the pressure of the hot-press sintering increases. When the hot-press sintering enters the sintering stage, the high compressive stress leads to effective plastic deformation and compaction results. It is reasonable to say that an increase in the sintering pressure contributes to the improvement of the crystal structure. As the experimental results showed, an increase of the sintering pressure increased

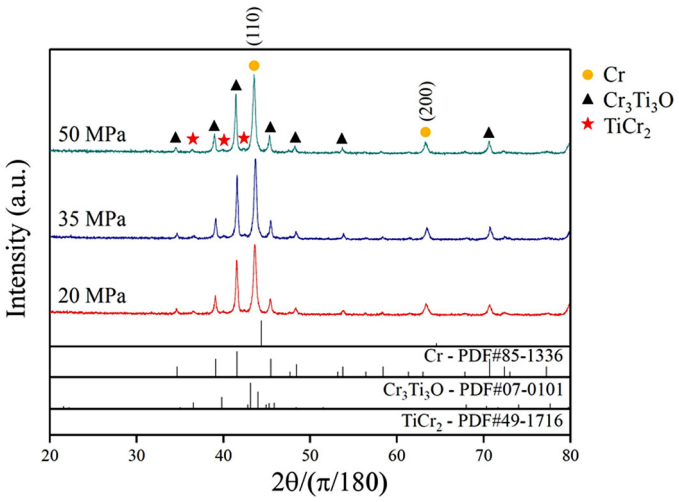

Fig. 1. XRD patterns of Cr-31.2 mass% Ti alloys by hot-press sintering at different pressures

the lattice diffraction of the unit area and enhanced the relative intensity. Therefore, when the hot-press sintering pressure was increased to 35 or 50 MPa, the major chromium phases could be compressed more efficiently and thereby a denser result achieved (Fig. 2b). In this study, the XRD patterns show that the major diffraction peaks appear in the Cr (110) and (200) planes, as shown in Figure 1. As the pressure increased (20 → 35 → 50 MPa), the

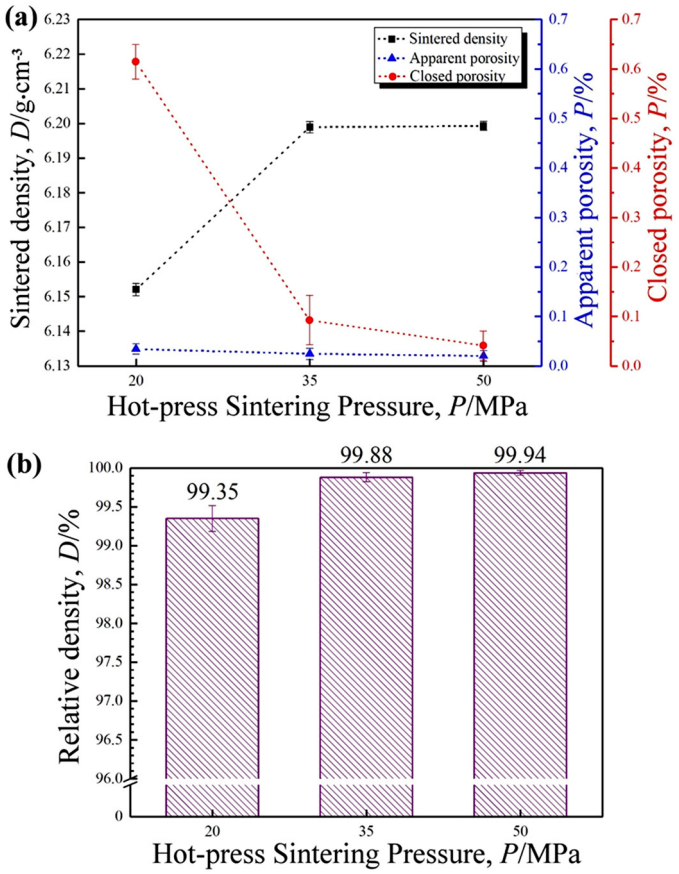

Fig. 2. Comparison of the properties of Cr-31.2 mass% Ti alloys by hot-press sintering at different pressures: (a) sintered density, apparent and closed porosities, and (b) relative density

intensity of the Cr diffractions (110) slightly increased. When the hot-press sintering pressure was increased, the chromium diffraction peak appeared toward the low-angle offset phenomenon. It was reasonable to suggest that the increased pressure effectively enhanced the solid-solution reaction between the chromium and titanium elements.

$TiCr_2$ and Cr_3Ti_3O diffraction peaks also appeared in the sintered specimens, since the high-activity titanium easily produced a chemical reaction with the oxide. Once the titanium oxide was formed, it immediately reacted with the chromium and the Cr_3Ti_3O phases were found. Besides, only a small amount of titanium and chromium was needed to generate the $TiCr_2$ phases. Increasing the hot-press pressure served to slightly increase the intensity of the Cr_3Ti_3O and effectively enhance the crystal structure of the Cr-31.2 mass% Ti alloys, further improving its mechanical characterization and properties of the Cr-31.2 mass% Ti alloys.

A comparison of the sintered density, apparent porosity, closed porosity and relative density of the Cr-31.2 mass% Ti alloys by hot-press sintering at different pressures is shown in Figure 2. According to sintering theory and a technological perspective, the porosities rapidly reduce and there is significant grain size growth during the final stages of the sintering process. In the experiment, the relative density is equal to $D/D_{th} \times 100\%$, where D is the sintered density and D_{th} is the theoretical density of the specimens, respectively. The highest sintered density (6.20 $g \cdot cm^{-3}$) occurs after hot-press sintering at 1250°C, 50 MPa for 1 h; while the lowest apparent porosity (0.021%) and closed porosity (0.04%) are also produced, as shown in Figure 2a. Clearly, as the hot-press pressure increased, the sintered microstructure and mechanical properties of the Cr-31.2 mass% Ti alloys are effectively improved. The apparent porosity slowly declined as the pressure of the hot-press sintering increased, and the closed porosity also showed an obvious downward trend. Generally speaking, in the final stage of hot-press sintering, porosity should be eliminated. It is reasonable to speculate that the sintering density of the Cr-31.2 mass% Ti alloys increased mainly due to the tight compaction of the chromium particles via the enhanced pressure.

The highest relative density (99.94%) of the Cr-31.2 mass% Ti alloys also appeared after hot-press sintering at 1250°C, 50 MPa for 1 h. The results also indicate that the hot-press sintering pressure increased only slightly improve the relative density of the specimens, as shown in Figure 2b. Meanwhile, the apparent porosity and closed porosity levels were inversely proportional to the relative density. Since the hot-press sintering temperature did not meet the liquid phase (1412°C) of the Cr-Ti alloy, it was not possible for Cr-31.2 mass% Ti alloys to reach the liquid-phase sintering (LPS) state. According to sintering theory, under an atmospheric pressure it was difficult to achieve a high density (>95%) of the sintered alloys for solid-phase sintering (SPS) [15]. The characteristics of the hot-press sintering process with the mixed powder were synchronously heated and pressed into the shape of a graphite mold. When hot-press sintering enters the sintering stage, the high compressive stress leads to

effective atomic diffusion, deformation and compaction results. According to the above the results and discussion, increasing the hot-press sintering pressure (20 → 50 MPa) effectively provided the driving force of the sintering mechanism and aided the atomic diffusion due to the external pressure.

Figure 3 shows the SEM morphology observations of the Cr-31.2 mass% Ti alloys after hot-press sintering at different pressures. The residual black pores (as the arrow indicates) are still present after hot-press sintering at 1250°C, 20 MPa for 1 h, as shown in Figure 3a. Owing to the SPS effects and tight compaction results, the internal pores decrease rapidly as the hot-press pressure increases (Figure 3b). Further, almost no internal pores exist after hot-press sintering at 1250°C, 50 MPa for 1 h, as shown in Figure 3c. This result is consistent with the porosity level, as shown in Figure 2a. The closed porosity was 0.04% after 50 MPa of hot-press sintering. In this study, the internal pores obviously decrease as the sintering pressure increased (20 → 35 → 50 MPa), as shown in Figure 3a-c. As previously noted, the decrease of porosities was mainly due to the deformation and complete compaction of the chromium particles via the enhanced pressure. As a result, increasing the hot-press sintering pressure was effective in improving the compaction of the Cr phases, which resulted in the decrease in pores in the final stage of densification. Figure 3 also shows that the chromium tended to coarsen slightly due to the solid diffusion of the high temperature (1250°C) and high pressure (50 MPa). A comparison of the average grain sizes of the Cr-31.2 mass% Ti alloys by hot-press sintering at different pressures is shown in Figure 4. The average grain size was measured using the linear intercept method [15]. As the hot-press sintering pressure increased (20 → 35 → 50 MPa), the average grain size gradually increased (4.29 → 4.48 → 5.06 μm). The grain coarsening phenomenon appeared in the Cr-31.2 mass% Ti alloys after high-pressure hot-press sintering, but the actual increase in average grain size was limited to only 0.77 μm (4.29 → 5.06 μm). As our previous studies indicated [15,18], rapid grain growth during the early stage of sintering has been found in many nano and submicron material systems, with extremely rapid grain growth easily generated during high-temperature and high-pressure sintering. As compared with Figure 3, the Cr-31.2 mass% Ti powders seemed to lose their submicron-scale characteristics after hot-press sintering. This finding was in agreement with our previous studies [18,23].

Figure 5a shows the TRS and hardness tests of the Cr-31.2 mass% Ti alloys by hot-press sintering at the different pressures. As the relative density increases, the higher density provides stronger binding to prevent the rupture mechanism of genera-

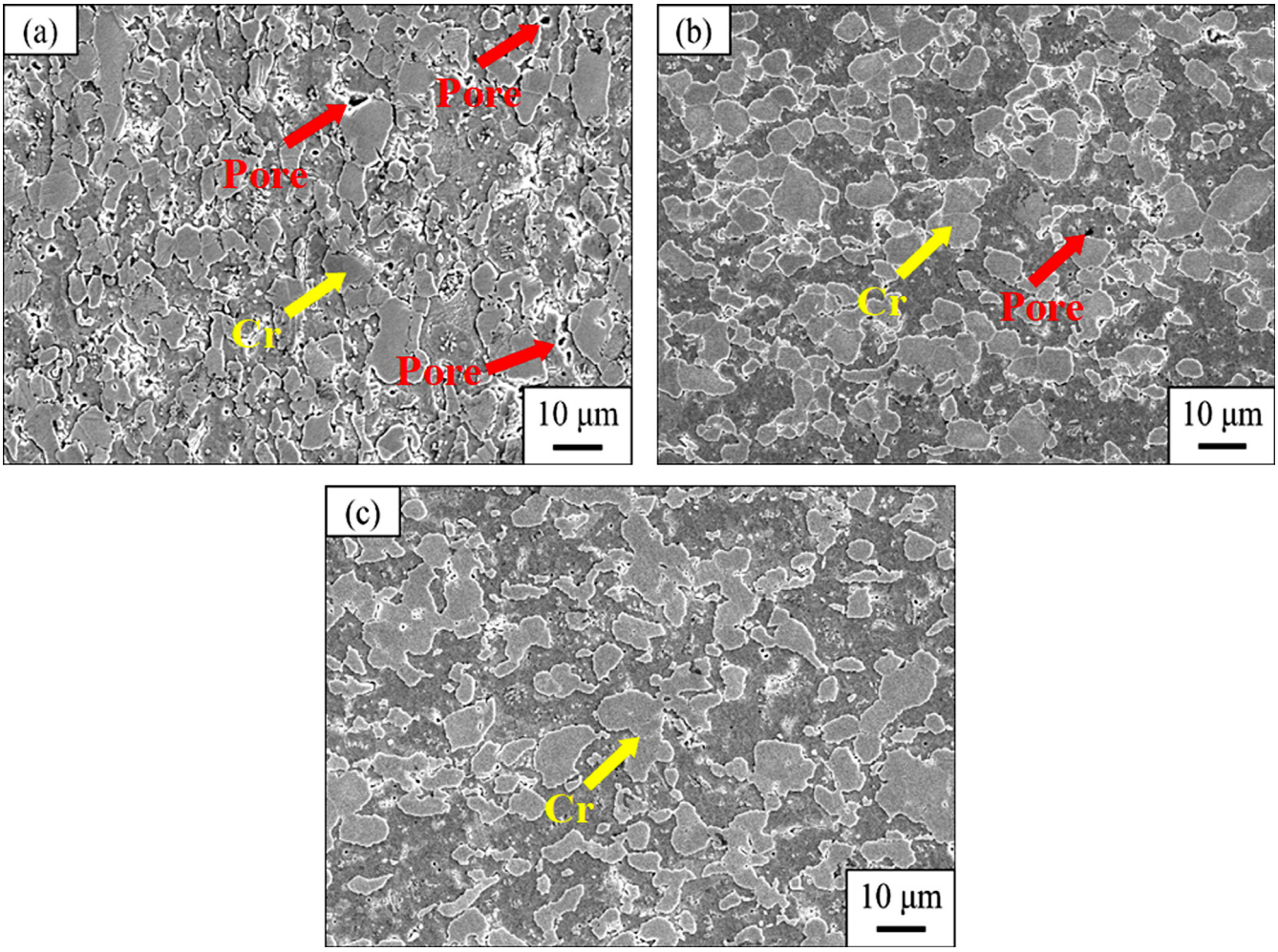

Fig. 3. SEM morphology observations of Cr-31.2 mass% Ti specimens by hot-press sintering at different pressures: (a) 20 MPa, (b) 35 MPa, and (c) 50 MPa

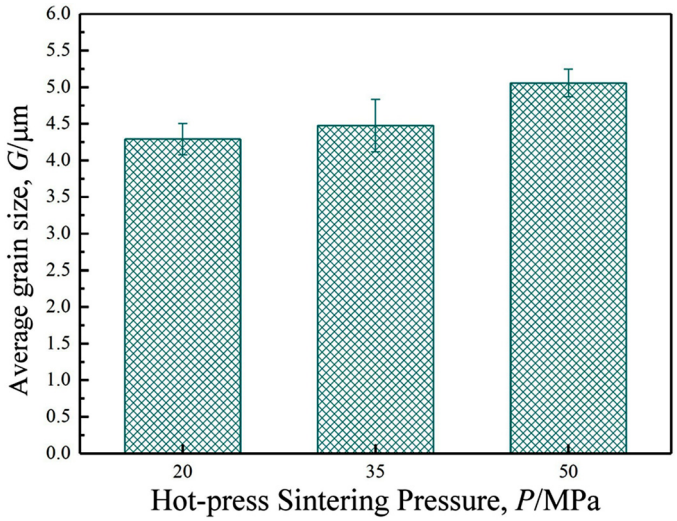

Fig. 4. Comparison of the average grain size of Cr-31.2 mass% Ti alloys by hot-press sintering at different pressures

tion. In the present research, increasing the pressure (20 → 35 → 50 MPa) of the hot-press sintering significantly improved the relative density (99.35 → 99.88% → 99.94%) of the Cr-31.2 mass% Ti alloys. The higher bonding strength, then hindered the generation of the rupture mechanism. In this work, the TRS values showed an increasing trend as the hot-press sintering pressure increased to 50 MPa. Although the average grain sizes showed a slight coarsening phenomenon after high-pressure sintering (50 MPa), the small variation in average grain size did not seem to affect the TRS value. The hot-press pressure and TRS values possessed a positive relationship, so the highest TRS value (448.53 MPa) appeared in the Cr-31.2 mass% Ti alloys after hot-press sintering at 1250°C and 50 MPa for 1 h.

In addition, the hardness values of the Cr-31.2 mass% Ti alloys are similar after the process of different hot-press sintering pressures, as shown in Figure 5a. Practically, the variation in hardness value is considered to be insignificant after different hot-press sintering pressures. Our previous studies revealed that decreasing the porosities of the sintered materials effectively enhanced plastic deformation resistance and hardness [16-18]. As seen in Figure 2b, the relative density is almost above 99.4% after hot-press sintering at different pressures. The average grain size increased only slightly as the pressure of the hot-press sintering increased. As the pressure increased (20 → 50 MPa), the change in hardness value was only from 81.87 to 81.90 HRA. As the sintered density and grain sizes were the important factors affecting the hardness of the Cr-31.2 mass% Ti alloys, it was another factor affecting the hardness as well. Previous literatures have indicated that hot-press sintering offers several advantages over conventional methods; primarily, the very low temperature required for densification [18,24,25]. When hot-press sintering enters the sintering stage (at a sufficiently high temperature), the high compressive stress leads to effective plastic deformation and compaction during the SPS step. Therefore, it is reasonable to suppose that the major differences in hardness result from the effects of the sintering density, SPS and grain size. In this study, the relative density and grain growth of the Cr-31.2 mass% Ti alloys did not show significant variations after the different sintering pressures. Other factors affecting hardness are plastic deformation and compaction during the SPS step. The results showed the hardness value to have only a slight variation. It is possible to say that the plastic deformation and compaction during the SPS step are not obviously different for various sintering pressures. In other words, when hot-press sintering enters the sintering stage, only a slight pressure is needed to achieve plastic deformation and compaction during the SPS step.

Cr-Ti alloys have been the object of great research interest due to their promising mechanical and electrical properties. Therefore, investigating the potential dependence of electrical conductivity through the Cr-Ti material is necessary. Generally, the electrical resistivity measurement is a useful tool when investigating the various phenomena in solids. It is an easy and inexpensive technique and can be used in the study of phase transformations, impurities, defects and other structural changes in crystal structure and amorphous metals/alloys. Figure 5b shows the electrical conductivity and sintered density of the Cr-31.2 mass% Ti alloys after hot-press sintering at different pressures. As the pressure increased, the sintered density rapidly increased and then maintained a value (6.20 g·cm^{-3}) in the range of 35 to 50 MPa. Our previous study has proven the relationship

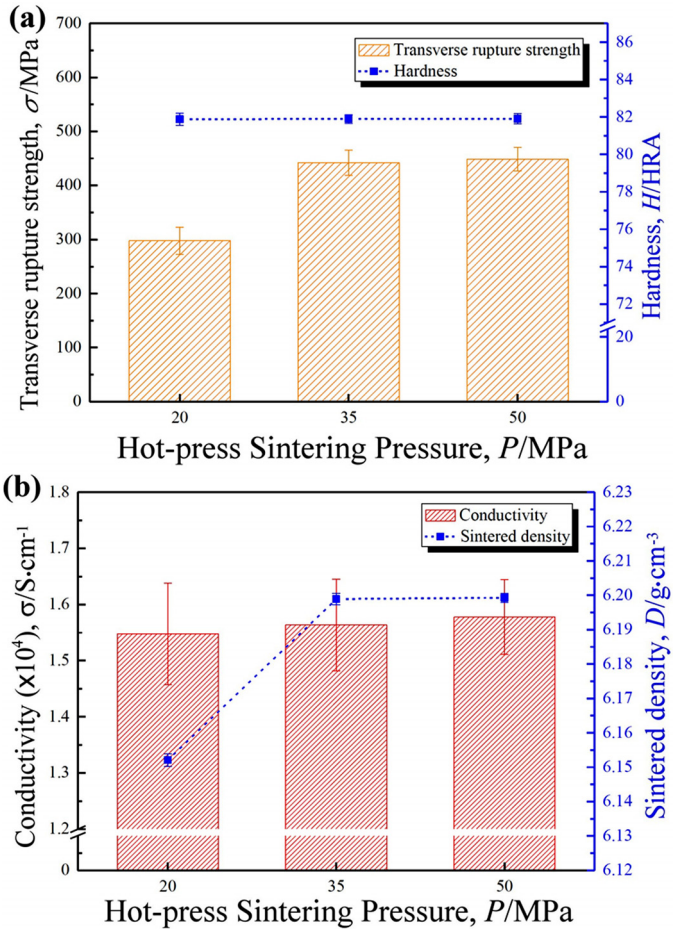

Fig. 5. Comparison of the mechanical and electrical tests of Cr-31.2 mass% Ti alloys by hot-press sintering at different pressures: (a) TRS and hardness test, and (b) conductivity test

of the relative density of Cr-based alloys to the electrical property. [16,18] Increasing the sintered density significantly improves the electrical conductivity of Cr-based alloys. The behaviors of the Cr-31.2 mass% Ti alloys were effectively improved as the hot-press sintering pressure increased. Meanwhile, the internal closed pores of the sintered specimens were significantly reduced after the high-pressure hot-press sintering treatments. As a result, the increase in sintering pressure enhanced the relative density and improved the electrical conductivity of the hot-press sintered Cr-31.2 mass% Ti alloys. The electrical conductivity rose only slightly as the pressure increased. The optimal electrical conductivity of $1.58 \times 104\ S \cdot cm^{-1}$ appeared after hot-press sintering at 1250°C and 50 MPa for 1 h.

Figure 6 shows the fractographic observations of the Cr-31.2 mass% Ti alloys after hot-press sintering at different pressures. It was found that obviously brittle fractographs existed in the Cr-31.2 mass% Ti alloys after the TRS tests. Residual pores are clearly apparent on the fracture surface, as indicated by the arrows in Figure 6a. These pores produced stress concentration points during the TRS test and result in a decline in fracture strength. As the pressure increases, the residual pores dramatically decrease, as shown in Figure 6b-c. Consequently, the fracture strength showed an obvious increase (297.73 → 442.19 → 448.53 MPa). As seen in Figure 7, the fracture mechanism of all specimens is evidenced by the cleavage fracture generated in the brittle chromium. When the deformation of a specimen exceeded its elastic limit, it cracked under the concentrated stress, causing the local chromium particles near the Cr-$TiCr_2$-Cr_3Ti_3O interfaces to spread and expand rapidly, which was detrimental to the fracture resistance of the interface. Our previous study [26] also showed that a small amount of the titanium and chromium formed $TiCr_2$ phases, while the XRD intensity of the $TiCr_2$ intermetallic peaks was weak. Moreover, the compounds like spinel Cr_3Ti_3O were not a significant variation as the hot-press sintering pressure increased. Thus, the Cr_3Ti_3O and $TiCr_2$ Laves phases could be not a main fracture mechanism affecting the TRS values. Though the brittle oxide was the main constituent of the Cr_3Ti_3O phase within the matrix of Cr-Ti alloy powders oxidized in the atmosphere [26], no evidence of it was found within the matrix generated a significant effect on the TRS. Thus, the Cr_3Ti_3O phase affects the evolution of TRS could be ignored. It was reasonable to speculate that the main fracture mechanism of the Cr-31.2 mass% Ti alloys was generated by the brittleness of the chromium.

Previous literature showed that a $TiCr_2$ phase with the Laves structure formed in binary Ti-Cr alloys when the Cr content

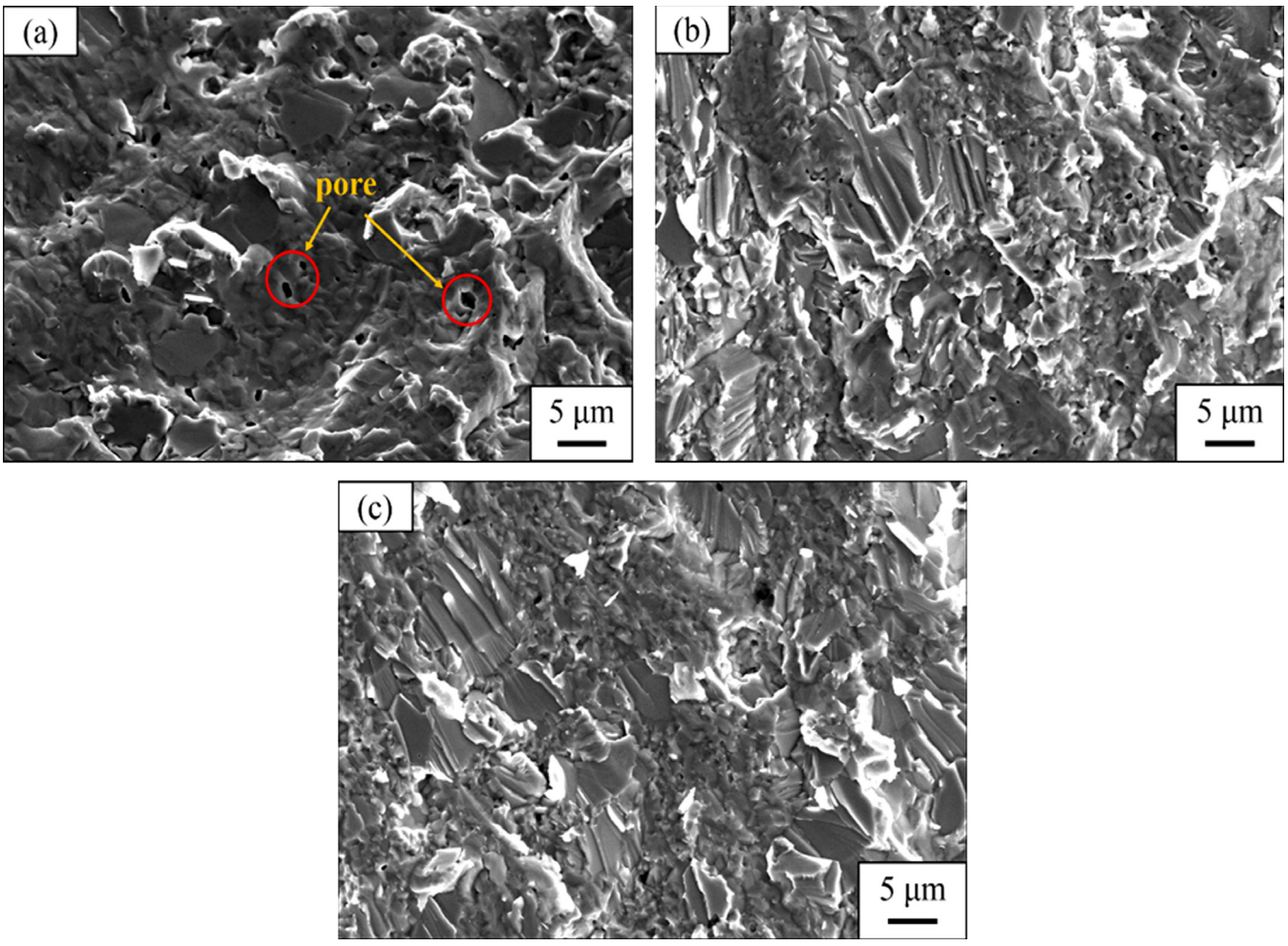

Fig. 6. Low-magnification fractographs observation of Cr-31.2 mass% Ti specimens by hot-press sintering at different pressures: (a) 20 MPa, (b) 35 MPa, and (c) 50 MPa

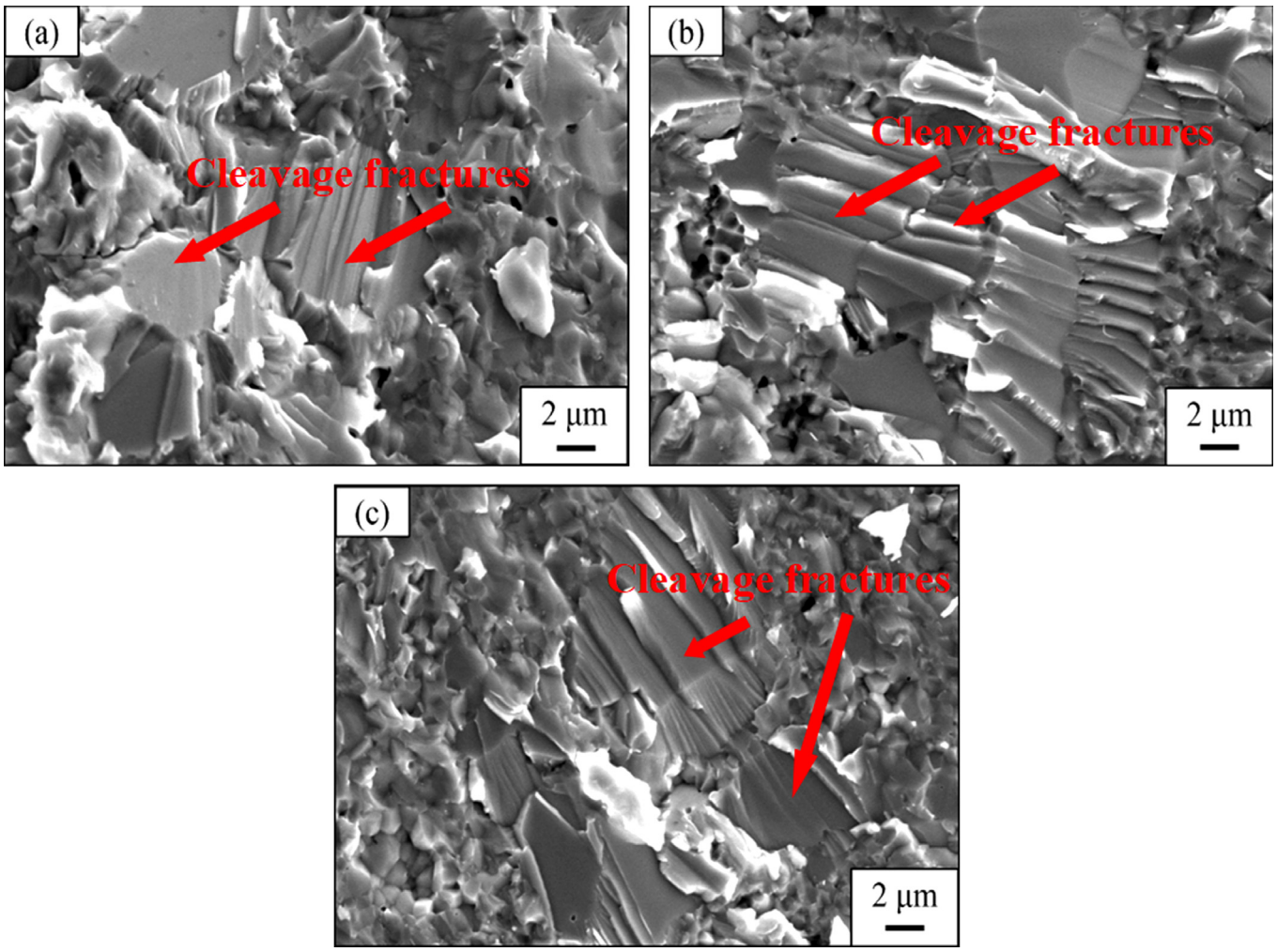

Fig. 7. High-magnification fractographs observation of Cr-31.2 mass% Ti specimens by hot-press sintering at different pressures: (a) 20 MPa, (b) 35 MPa, and (c) 50 MPa

was higher than 15% [4]. Moreover, the microstructure and mechanical properties of these alloys are very sensitive to their Cr content and preparation procedures. In this study, as the ratio of chromium is up to 68.8 mass%, the x-ray analysis shows that the major Cr phases and minor $TiCr_2$ phase are clearly produced after hot pressing with different pressures (as shown in Figure 1). It is reasonable to speculate that the main fracture mechanism of the Cr-31.2 mass% Ti alloys is generated by the brittle properties of the chromium, which shows obvious cleavage fractures, stepped cleavage planes and relatively flat fracture planes, as shown in Figure 7. It was possible to say that more cleavage fractures appeared in the microstructures of the Cr-31.2 mass% Ti alloys and easily resulted in a lower TRS value. According to above discussion and results, the hot-press sintering parameters of 1250°C at 50 MPa for 1 h for the Cr-31.2 mass% Ti alloys achieved the optimal mechanical and electrical properties.

In addition, our previous study indicated that the particle size of steel powders greatly affects the grain size of sintered bodies through the sintering process, and that using a smaller size of steel powders to decrease the average grain size effectively improved the hardness and TRS results [27]. Fe-base powder metallurgy was consolidated by the hot press process aim for increasing its strength and hardness through distribution of the fine grain [28]. In this study, we also mixed submicron-structured titanium (760 nm) and chromium (588 nm) powders mixed to fabricate Cr-31.2 mass% Ti alloys via hot-press sintering at 1250°C and 50 MPa for 1 h. As seen in Figure 8a, the low magnification of the SEM morphology observations uncovers a significant agglomeration phenomenon in the sintered specimens. High-magnification SEM observations and the EDS analysis, as shown in Figure 8b, revealed the bulge in the granular structure to be mainly the solid-solution reaction of the chromium and titanium phases. The composition ratio of chromium and titanium is 85:15 (points 1 and 2), as shown in Table 1. Points 3 and 4 were the solid diffusion of the titanium phases, while points 5, 6 and 7 revealed a composition ratio of chromium and titanium of about 2:1, a typical ratio of the $TiCr_2$ Laves phase. As a result, it was reasonable to suggest that the major component of the matrix phases was the $TiCr_2$ intermetallic compound. This result is further compared with the properties of the micron- and submicron-structured Cr powders of the Cr-31.2 mass% Ti alloys after hot-press sintering at 1250°C, 50 MPa for 1 h, as shown in Table 2. Most of the sintered characteristics are similar, including the sintered

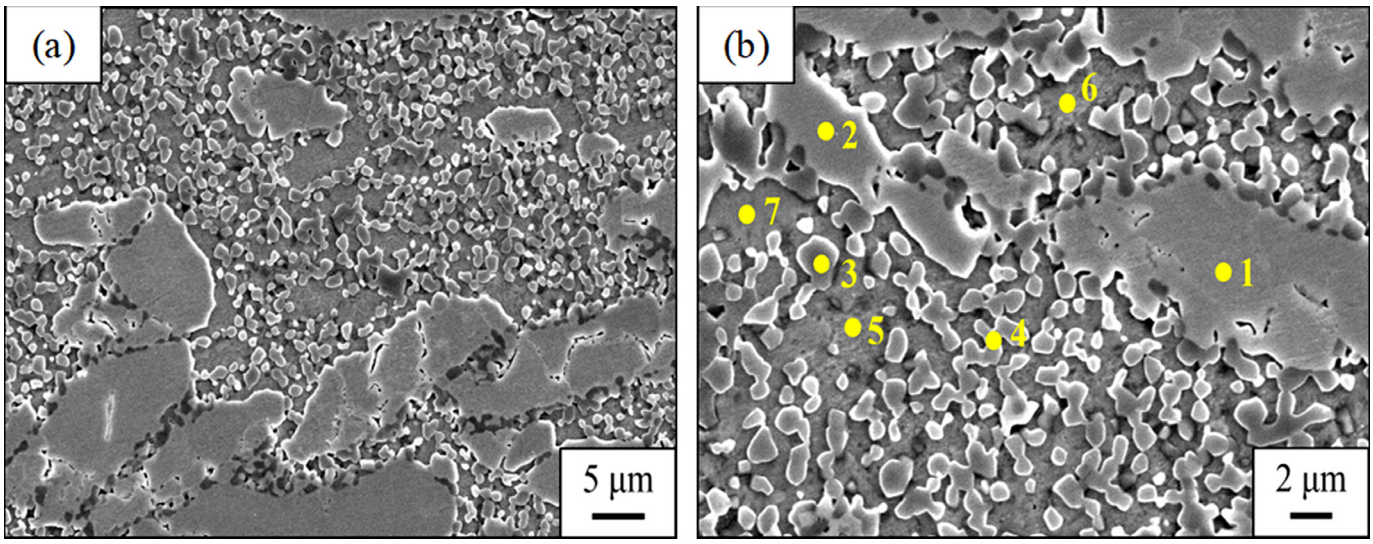

Fig. 8. SEM morphology observations of Cr-31.2 mass% Ti alloys produced by submicron-sized Ti and Cr powders after hot-press sintering at 1250°C, 50 MPa for 1 h: (a) low, (b) high-magnification

density and apparent porosity. Since the submicron-structured Cr powders possessed a smaller particle size, the sintered average grain size of the submicron-structured Cr powders was obviously smaller than that of the micron-structured Cr powders after hot-press sintering, at only 0.91 μm. The closed porosity was also relatively low (0.02%).

TABLE 1

EDS analysis of Figure 8 of Cr-31.2 mass% Ti alloys produced by submicron-sized Ti and Cr powders after hot-press sintering at 1250°C and 50 MPa for 1 h

Position	1	2	3	4	5	6	7
Cr (mass%)	85.3	85.4	14.0	11.5	65.0	66.6	67.3
Ti (mass%)	14.7	14.6	86.0	88.5	35.0	33.4	32.7

In the submicron-structured Cr and Ti powders hot-press sintering study, the formation of the $TiCr_2$ Laves phase was the major component of the matrix phases, which should be a contributor to the variation in hardness. A previous study has indicated that the $TiCr_2$ phase composition significantly affects the material properties. [4] As a result, a submicron-structured Cr powders of the Cr-31.2 mass% Ti alloys possessed a higher hardness value (83.23 HRA). However, the agglomeration phenomenon of the Cr phase and the brittleness of the $TiCr_2$ Laves phases could lead to the lower fracture strength, with the TRS decreasing slightly to 400.54 MPa.

In addition, the electrical conductivity also showed a slight decline to 1.50×10^4 S·cm^{-1}. Accordingly, the effective compaction of the submicron-structured Cr and Ti powders resulted in their good mechanical and electrical properties. The submicron-structured Cr powders of the Cr-31.2 mass% Ti alloys possessed a relatively smaller average grain size and higher hardness. This study confirmed that the hot-pressing technique processes were effective in improving the sintering mechanical properties and its characterization of Cr-31.2 mass% Ti alloys.

4. Conclusions

This study showed hot-press sintering to have a positive influence on the sintering behavior and to improve the performance of Cr-31.2 mass% Ti alloys. The optimal SPS process effectively eliminated the internal pores of the Cr-31.2 mass% Ti alloys (closed porosity of 0.04%), which resulted in ideal mechanical and electrical performances. Increasing the pressure (20 → 50 MPa) of the hot-press sintering process increased the relative density (99.35 → 99.94%) and electrical conductivity ($1.55 \times 10^4 \rightarrow 1.58 \times 10^4$ S·cm^{-1}). Moreover, a higher hardness (81.90 HRA) and the highest TRS value (448.53 MPa) were obtained.

The submicron-structured titanium (760 nm) and chromium (588 nm) powders were used to fabricate Cr-31.2 mass% Ti alloys via hot-press sintering at 1250°C and 50 MPa for 1 h.

TABLE 2

Comparison of the properties of micron and submicron-structured Cr powders of Cr-31.2 mass% Ti alloys after hot-press sintering at 1250°C and 50 MPa for 1 h

Mean particle size of Cr powders	Sintered density (g·cm^{-3})	Apparent porosity (%)	Closed porosity (%)	Grain size (μm)	Electrical conductivity (×10^4 S·cm^{-1})	Hardness (HRA)	TRS (MPa)
4.66 μm	6.20	0.021±0.011	0.04±0.03	5.06±0.19	1.58±0.07	81.90±0.27	448.53±21.61
588 nm	6.16	0.024±0.007	0.02±0.02	0.91±0.15	1.50±0.08	83.23±0.25	400.54±23.52

The result was the more effective compaction of the submicron-structured Cr and Ti powders of the Cr-31.2 mass% Ti alloys (closed porosity of 0.02%) and the highest hardness value of 83.23 HRA. However, the agglomeration phenomenon of the Cr phase and brittleness of the $TiCr_2$ Laves phase, Cr-31.2 mass% Ti alloys were performed the suitable sintering parameters to enhance electrical conductivity a slight decline to $1.50 \times 10^4\,S \cdot cm^{-1}$ and an impressive substrate matrix with a high-density value of 99.94%.

Acknowledgments

This research is supported by the ASSAB STEELS TAIWAN CO., LTD. The authors would like to express their appreciation for Dr. Harvard Chen, Michael Liao and Mr. Meng-Yu Liu.

REFERENCE

[1] B. Mallia, P.A. Dearnley, Wear **263**, 679-690 (2007).
[2] H.C. Hsu, S.C. Wu, C.F. Wang, W.F. Ho, J. Alloys Compd. **487**, 439-444 (2009).
[3] X. Zhao, M. Niinomi, M. Nakai, J. Hied, T. Ishimoto, T. Nakano, Acta Biomater. **8**, 2392-2400 (2012).
[4] Y.Z. Zhang, C. Meacock, R. Vilar, Mater. Des. **31**, 3891-3895 (2012).
[5] Y.Q. Hu, H.F. Zhang, C. Yan, L. Ye, B.Z. Ding, Z.Q. Hu, Mater. Lett. **58**, 783-786 (2004).
[6] Q. Yao, J. Sun, D. Lin, S. Liu, B. Jiang, Intermetallics **15**, 694-699 (2007).
[7] B. Mallia, P.A. Dearnley, Wear **263** (1-6), 679-690 (2007).
[8] M.A. Ezazi, Ceram. Int. **40** (10), 15603-15615 (2014).
[9] S. Amira, Intermetallics **18** (1), 140-144 (2010).
[10] L. Bolzonia, I. Montealegre Meléndez, E.M. Ruiz-Navas, E. Gordo, Mater. Sci. Eng. A **546**, 189-197 (2012).
[11] X.M. Duan, D.C. Jia, Z.L. Wu, Z. Tian, Z.H. Yang, S.J. Wang, Y. Zhou, Scripta Mater. **68**, 104-107 (2013).
[12] Q.G. Li, Z. Wang, C. Wu ,X. Cheng, J. Alloys Compd. **640**, 275-279 (2015).
[13] L. Bolzoni, E.M. Ruiz-Navas, E. Neubauer, E. Gordo, Mater. Chem. Phys. **131**, 672-679 (2012).
[14] Z.H. Qiao, X.F. Ma, W. Zhao, H.G. Tang, B. Zhao, J. Alloys Compd. **462**, 416-420 (2008).
[15] S.H. Chang, C.L. Liao, K.T. Huang, M.W. Wu, Mater. Trans. **57**, 732-737 (2016).
[16] S.H. Chang, C. Liang, J.R. Huang, K.T. Huang, Powder Metall. **59**, 142-147 (2016).
[17] S.H. Chang, P.Y. Chang, Mater. Sci. Eng. A **606**, 150-156 (2014).
[18] C. Liang, S.H. Chang, J.R. Huang, K.T. Huang, S.T. Lin, Mater. Trans. **56**, 1127-1132 (2015).
[19] P. Zhou, Y.B. Peng, B. Hu, S.H. Liu, Y. Du, S.Q. Wang, G.H. Wen, W. Xie, CALPHAD **41**, 42-49 (2013).
[20] W. Tillmann, A. Fehr, M. Ferreira, D. Stangier, Int. J. of Refract. Met. and Hard Mater. **73**, 146-156 (2018)
[21] K. Kashimura, J. Fukushima, T. Mitani, M. Sato, N. Shinohara, J. of Alloys and Compd. **550**, 239-244 (2013).
[22] Y. Sun, W. Zeng, Y. Zhong, M. Wang, H. Liu, G. Cai, Z. Jin, Thermochim. Acta **652**, 24-33 (2017).
[23] S.H. Chang, M.H. Chang, K.T. Huang, J. Alloys Compd. **649**, 89-95 (2015).
[24] X.F. Zhao, Y.C. Teng, H. Yang, Y. Huang, J.Y. Ma, Ceram. Int. **41**, 11062-11068 (2015).
[25] X. Zhou, M.G. Wang, H.C. Zhao, J. Alloys Compd. **665**, 100-106 (2016).
[26] S.H. Chang, C.L. Li, K.T. Huang, Mater. Trans. **58**, 1190-1196 (2017).
[27] K.T. Huang, S.H. Chang, M.W. Wu, C.K. Wang, ISIJ Int. **56**, 335-340 (2016).
[28] J. Konstanty, D. Tyrala, A. Radziszewska, Arch. Metall. Mater. **54** (4), 1051-1058 (2009).